Origin, Evolution, and Imaging of Vortices in Atomic Processes

J. H. Macek
Department of Physics and Astronomy, University of Tennessee, Knoxville, Tennessee 37996, USA and Physics Division, Oak Ridge National Laboratory, Oak Ridge, Tennessee 37831, USA

J. B. Sternberg and S. Y. Ovchinnikov*
Department of Physics and Astronomy, University of Tennessee, Knoxville, Tennessee 37996, USA

Teck-Ghee Lee and D. R. Schultz
Physics Division, Oak Ridge National Laboratory, Oak Ridge, Tennessee 37831, USA
(Received 10 October 2008; published 10 April 2009)

Vortices are usually associated with systems containing large numbers of particles. Of particular topical interest though are those formed within atomic-scale wave functions and observed in macroscopic systems such as superfluids and quantum condensates. We uncover them here in one of the most fundamental quantum systems consisting of just one electron and two protons. Moreover, the results of novel simulations of the dynamics of this system reveal previously unknown mechanisms of angular momentum transfer and new ways to image atomic-scale quantized vortices at macroscopic distances. Probing of vortices and vortex-driven dynamics in quantum systems is thereby illustrated.

DOI: 10.1103/PhysRevLett.102.143201 PACS numbers: 34.50.Fa

Vortices, fascinating topological objects, are ubiquitous in nature. Their origin, geometries, and interactions are particularly important for understanding the dynamics of phase transitions in the laboratory and the Universe [1], leading to an intense cross-fertilization of fields of science. Since their discovery in quantum systems [2] they have been visualized in various experiments [3–5] and shown by theoretical calculations [6,7].

Here we uncover unexpected vortices in the electronic wave function in the prototypical quantum system consisting of a single electron in the field of two moving protons. In particular, we show how vortices appear in this system, rotate around the nuclei, and interact, thereby transferring angular momentum from nuclear to electronic motions, casting new light on how angular momentum is transferred in atomic-scale interactions. While earlier theories [1,2,6,7] showed that vortices in single-particle wave functions are consistent with the time-dependent Schrödinger equation, they have not shown how such vortices can be formed in realistic physical systems nor how they can be observed experimentally. In addition, previous observations of vortices have involved large numbers of particles and therefore do not address the formation of vortices in single-particle wave functions [2].

In this Letter we show that when the final atomic states form in this prototypical single-particle wave function, some vortices become pinned to the atomic centers but others unexpectedly remain in the continuum. These vortices eventually appear as zeros in the momentum distributions of ionized electrons and could be observed with state-of-the-art, reaction microscope measurements [8,9]. While vortices corresponding to oriented bound states of atoms have been discussed [10], the essential outcome of the work reported here is that vortices are also formed in continuum states but are not bound to a charge center. In this sense they are ''free'' vortices. The observation of such vortices in simple systems is of fundamental importance and would directly confirm their presence in time-dependent quantum processes. In addition, further theoretical exploration will elucidate the connection with physical phenomena such as angular momentum transfer.

Even though the static properties of H_2^+ have been known since the early days of quantum mechanics, accurate simulation of dynamical breakup, or ionization, in $H^+ + H$ remains a theoretical challenge despite our complete knowledge of the relevant interactions. The simulations are challenging because of highly oscillatory exponential phase factors in the electronic wave function and the infinitesimally small values of the continuum components of electronic probability density at large times after the collision. The approach we recently developed [11] addresses these difficulties by removing the diverging phase factors from the electronic wave function $\psi(\mathbf{r}, t)$, where $\mathbf{r}$ is the electronic coordinates and t is the time, and transforming the time-dependent Schrödinger equation to an expanding space. With removal of the diverging phase factor the regularized wave function $\Phi(\mathbf{q}, \tau)$ satisfies the regularized time-dependent Schrödinger equation (RTDSE)

$$\left[-\frac{1}{2}\nabla_{\mathbf{q}}^2 + \frac{1}{2}\Omega^2 q^2 + R^2 V(\mathbf{q}, \tau)\right]\Phi(\mathbf{q}, \tau) = i\frac{\partial \Phi(\mathbf{q}, \tau)}{\partial \tau}, \tag{1}$$

where $\mathbf{q} = \mathbf{r}/R$ are the coordinates in the expanding space, $R = R(\tau)$ is the expanding scale, τ is the scaled time ($d\tau = dt/R^2$), $\Omega = \Omega(\tau) = Rd(R^{-2}dR/d\tau)d\tau$, and $V(\mathbf{q}, \tau)$ is

the potential in the expanding space. The RTDSE is then solved efficiently using well-established numerical lattice methods [12]. In the present calculation we use $R(\tau)$ as the distance between the two protons, and we note that $|\psi(\mathbf{r}, t)| = |\Phi(\mathbf{q}, \tau)|$ given the coordinate transformation defined above.

To trace the origins of the vortex formation and dynamics, we computed the electronic wave function for proton-hydrogen collisions at 5 keV of impact energy and an impact parameter, b, of 1 a.u. Vortices first form when the separation between the projectile and the target is $R \approx 5$ a.u. (Fig. 1) and are associated with a sudden change of topology of the classically allowed region of electron motion. Initially, when the protons are far apart, the topology of the classically allowed region is that of isolated atoms. Then during the collision, the potential barrier separating the two attractive Coulomb wells drops below the atomic eigenenergy, allowing the electron to move around the two atomic nuclei so that the classically allowed region has a molecular topology. This sudden change induces $1s\sigma_g - 3d\sigma_g$ transitions [13] that give rise to $3d\sigma_g$ [14] nodal surfaces in the time-dependent electronic wave function seen as nodal lines in Fig. 1(a). The nodal structures are precursors to vortex formation as discussed initially by Dirac [2] and applied later by others [7].

At slightly later times, when $R = 4.8$ a.u., a vortex separates from the nodal surface, seen in Fig. 1(b). This vortex is not associated with any center of force (i.e., neither proton). Here the electronic density locally circulates around a vortex center, indicated by the arrows pointing along the electronic probability current in Fig. 1(b′). This current circulation is a physical consequence of transferring angular momentum from relative to internal motion of the atoms. The electronic density rotates about the center of the vortex and, in turn, the center of the tornado-like vortex itself rotates around the quasimolecule (Fig. 2) and transfers angular momentum to the electron.

Our computations also reveal another new topological feature, namely, ring vortices, analogous to classical smoke rings, which appear and disappear during the collision. Ring vortices have been discussed in Ref. [6] in the context of coherent superpositions of atomic states. The present ring vortices are associated with the superposition of ''united atom'' states. The united atom states have a similar topology to that of atomic states where both protons are screened by a centrifugal potential and the electron perceives the protons as a single (''united'') Coulomb center. The united atom topology only exists for a short time; therefore the ring vortices also exist for the same period of time. These states are populated by recapture from continuum adiabatic states formed on the incoming phase of the collision. The distances where the ring vortices are formed coincide with distances $R = l(l + 1)/2$ [13] where transitions from continuum to bound states occur. These distances are determined by the united atom orbital quantum numbers with $l > 0$. The ring vortex shown in Fig. 2(b) corresponds to $l = 3$.

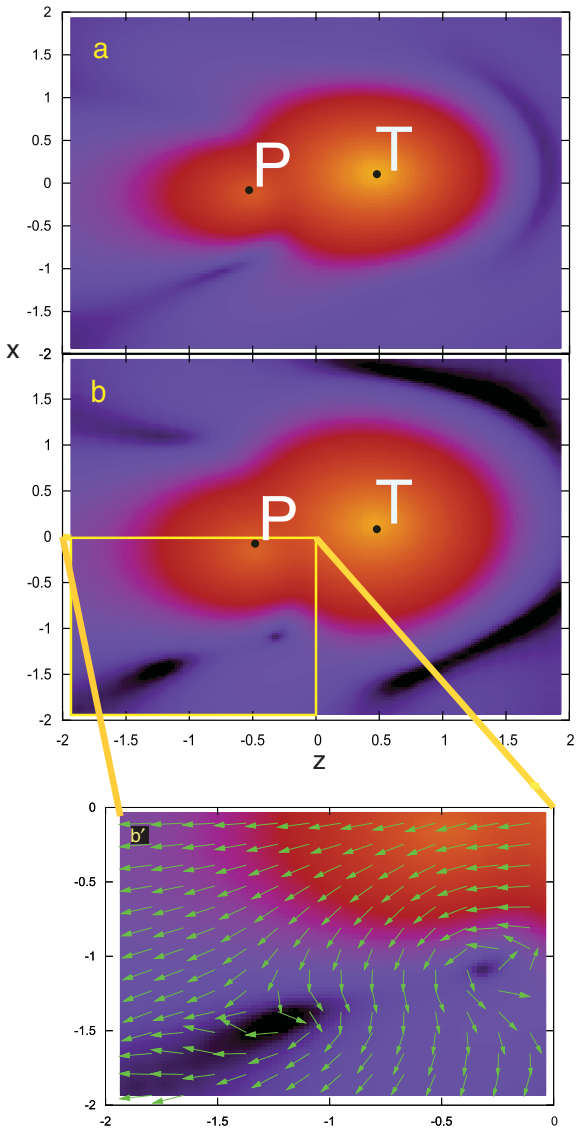

FIG. 1 (color). Vortex origin. (a) Density plot of the electronic wave function $|\Phi(\mathbf{q}, \tau)|$, $\mathbf{q} = (x, y, z)$, at $R = 5$ a.u. in scaled coordinates $\boldsymbol{q}$. All of the coordinates are scaled by the internuclear distance R and the coordinate axis z is parallel to the approaching proton's initial velocity. The nucleus of the target (T) is centered at $q_z = 1/2$ and the projectile (P) is centered at $q_z = -1/2$. The bright areas indicate high electronic probability density and the dark areas low. The nodal lines are seen as the dark, linear features to the left of the projectile in these figures. (b) At $R = 4.8$ a.u. a hole, visible in the lower left-hand boxed quadrant, has separated from the nodal line. (b′) Arrows represent the electronic probability current.

The expanding ring vortices entangle with the rotating tornado vortex [Fig. 2(c)] and are later absorbed by the tornado [Fig. 2(e)] as illustrated schematically in Fig. 2(c′). Figure 2(f) shows the presence of several vortices at an intermediate, postcollision distance of $R = 50$ a.u. At these distances the electronic wave function has a π-type distribution of H_2^+ with a nodal line running between the protons.

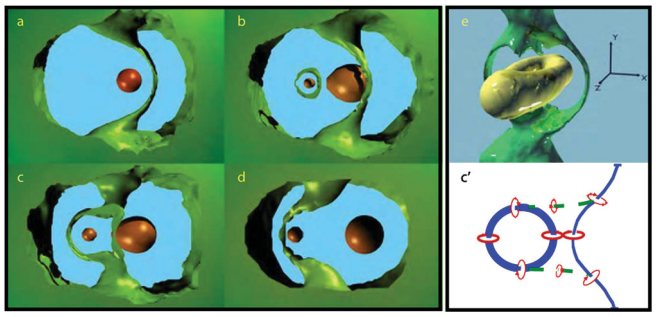

FIG. 2 (color). A "tornado" vortex. (a)–(d) show a cut (blue plane) through a three-dimensional representation of the time-dependent wave function. The gold surface represents the maxima of $|\Phi(\mathbf{q}, \tau)|$ and the green surface represents the minimum. (a) The tornadolike structure bends around the target atom (at the center of the gold surface), in the receding phase of the collision at $R = 5.8$ a.u.. (b) At $R = 6.1$ a.u., a vortex ring forms around but away from the projectile center (at the center of the other gold surface) while the tornado has rotated slightly. (c) The tornado and vortex ring entangle at $R = 6.2$ a.u. and the tornado absorbs the ring. (d) At $R = 6.3$ a.u. the tornado has rotated to a new position around the projectile and the vortex ring has been absorbed. (c′) A schematic plot of the ring and tornado vortex collision and the associated current circulation. In order to maintain continuous current circulation, they connect along the dashed lines. In the region between the upper and lower dashed lines the currents rotate in opposite directions; thus, this portion of the vortices annihilates and only the tornadolike vortex remains. (e) Vortices at $R = 50$ a.u. (postcollision) showing two tornado vortices encircling the yellow torus and two less noticeable tornados pointing down toward the torus. The x-z plane is the collision plane.

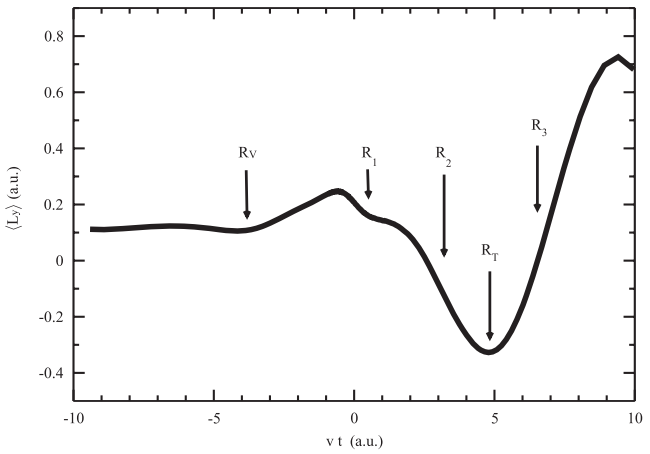

FIG. 3. The mean value of the electron angular momentum perpendicular to the collision plane $\langle L_y \rangle$ is shown as a function of time. In the absence of vortices, the curve would be approximately constant at the initial value $b\upsilon/4 = 0.112$, where υ is the collision velocity, 0.447 a.u. Structures in the curves are related to vortex dynamics as described in the text.

When the final atomic bound states are formed, several tornado vortices appear and some of them become pinned to atomic centers. These pinned vortices are associated with bound states that have nonzero projections of angular momentum on an axis perpendicular to the scattering plane, implying that angular momentum is ultimately transferred to circulation about one or the other proton; that is, the atomic states have nonzero orientation parameters [15]. Such parameters have been measured for several atomic processes [10] and, in light of the present results, provide indirect evidence of vortex motion in simple atomic systems. Further, the typical picture of collisional orientation, as summarized, for example, in "propensity rules" [16], envisions that electron distributions circulate about atomic centers without prior circulation about free vortex centers. In contrast, our computations show that the transfer of angular momentum sets up local circulation about the center of free vortices and initiates rotational motion seen as orientation of atomic states.

For example, the vortices change the mean value of the electronic angular momentum perpendicular to the collision (x-z) plane, namely, $\langle L_y \rangle$ seen as a function of time in Fig. 3. Without the vortices, this plot would show an approximately constant value. The curve has considerable structure and is related to the first vortex formation at R_V, angular momentum transfer due to united atom rotational coupling at $t = 0$, and the formation, at R_T, of the top-of-barrier component [8,11,17] which evolves to the π-state distribution seen in Fig. 2(f). At these points the mean angular momentum transfer changes character either increasing as at R_V and R_T or decreasing as at $t = 0$. In contrast the appearance of ring vortices at R_i, $i = 1, 2, 3$, does not affect the transfer of angular momentum since they carry no net angular momentum.

Even though free vortex motion is consistent with quantum mechanics [6], no examples of free vortices in actual physical systems have been observed. Vortices in many-particle systems are observed by direct imaging, as in the recent case of Bose-Einstein condensates (BECs) [4,5], where they are visually observed by light scattering or absorption. This is possible because the condensate is a macroscopic many-particle system. No similar imaging has been proposed for atomic-scale, single-particle quantum wave functions, yet direct observation of vortices in such systems would greatly extend our understanding of quantized vortices.

To visualize vortices, we use an "imaging" theorem based on fundamental results regarding the time evolution of quantum systems [17]. When the wave function for a particle initially localized in some bounded region of space is released to move in the absence of forces, then the wave function expands linearly with time. This implies that the probability density $P(\mathbf{r}, t) = |\psi(\mathbf{r}, t)|^2$ becomes proportional to the momentum distribution $P(\mathbf{k})$ for detecting an electron with momentum $\mathbf{k} = \mathbf{r}/t$ in the limit of kt being asymptotically large compared with the mean dimensions of the initial state. This connection between the observable momentum distribution and the time-dependent wave function implies that vortices in the wave function at

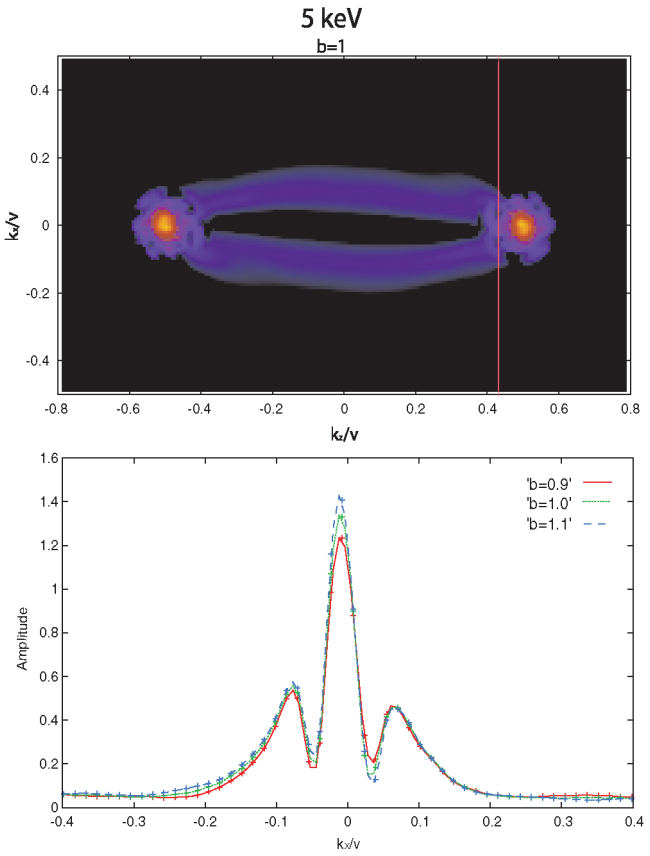

FIG. 4 (color). Logarithmic contour plot of the electron momentum distribution $\sqrt{P(\mathbf{k})}$ at $b = 1$ in the collision plane showing dark holes corresponding to vortices in the atomic wave function. The lower plot is a linear plot of a slice of the distribution through two vortices at three impact parameters near $b = 1$.

large times can be imaged, for example, using contemporary reaction microscope techniques [8,9].

Here, the evolution of the electronic wave function and vortices was followed to internuclear distances of $R = 10^6$ a.u. or 50 μm. Thus, the momentum distribution $P(\mathbf{k})$ images the continuum wave function, with free vortices appearing as holes, seen in Fig. 4. To demonstrate that the vortices will be present in the full momentum distribution, also shown is a plot of $\sqrt{P(\mathbf{k})}$ along a slice of the contour plot at $k_y/v = 0$, $k_z/v = 0.437$ for varying k_x showing that the vortex structures at $k_x/v = -0.05$ and $+0.04$ are fairly insensitive to the impact parameter. Observation of these structures would unambiguously confirm the importance of vortex theory in quantum mechanics.

We note that quantized vortices are a common phenomena in BECs and in superfuilds such as liquid helium. Here we see that these phenomena also occur in single-particle quantum systems described by a linear partial differential equation, namely, the Schrödinger equation with no nonlinear terms as are present in the Gross-Piteavskii equation describing BECs. Our calculations serve as a model for the dynamics of vortices in atomic systems, and show that such vortices remain when systems evolve to macroscopic distances where they can be imaged. The present study may thereby open up a new way to explore turbulence in quantum systems. Of particular interest in this comparison are the dynamics of vortices created via collisions of two species including BECs.

Finally, the present work has revealed that vortex motion is a heretofore unrecognized characteristic of atomic-scale dynamics and that vortices may play a role in correlated dynamics that have been difficult to interpret with conventional pictures. It shows that vortices in single-electron wave functions can be directly observed experimentally, elucidates the origin of vortices in dynamic systems, and shows that they play an important role in angular momentum transfer. Thus, the work reported here opens up a path towards a new perspective on a very broad range of atomic-scale physics.

This research is sponsored by the Office of Basic Energy Sciences, U.S. Department of Energy, through grants to the University of Tennessee (DE-FG02-02ER15283) and the Oak Ridge National Laboratory which is managed by UT-Battelle, LLC under Contract No. DE-AC05-00OR22725.

*Permanent address: Ioffe Physical Technical Institute, St. Petersburg, Russia.

[1] L. M. Pismen, *Vortices in Nonlinear Fields: From Liquid Crystals to Superfluids, From Non-Equilibrium Patterns to Cosmic Strings* (Oxford University, Oxford, 1999).
[2] E. Schrödinger, Phys. Rev. **28**, 1049 (1926); P. A. M. Dirac, Proc. R. Soc. A **133**, 60 (1931).
[3] K. W. Madison *et al.*, Phys. Rev. Lett. **84**, 806 (2000).
[4] J. R. Abo-Shaeer, Science **292**, 476 (2001).
[5] M. W. Zwierlein, Nature (London) **435**, 1047 (2005).
[6] I. Bialynicki-Birula, Z. Bialynicka-Birula, and C. Sliwa, Phys. Rev. A **61**, 032110 (2000).
[7] J. O. Hirschfelder, C. J. Goebel, and L. W. Bruch, J. Chem. Phys. **61**, 5456 (1974).
[8] R. Dörner *et al.*, Phys. Rev. Lett. **77**, 4520 (1996).
[9] J. Ullrich *et al.*, Rep. Prog. Phys. **66**, 1463 (2003).
[10] N. Andersen *et al.*, Phys. Rep. **278**, 107 (1997).
[11] T.-G. Lee *et al.*, Phys. Rev. A, **76**, 050701(R) (2007).
[12] D. R. Schultz, M. R. Strayer, and J. C. Wells, Phys. Rev. Lett. **82**, 3976 (1999).
[13] S. Yu. Ovchinnikov and E. A. Solov'ev, Sov. Phys. JETP **64**, 280 (1987).
[14] To classify adiabatic states we use spherical quantum numbers of the united atom and their spectroscopic notations.
[15] U. Fano and J. H. Macek, Rev. Mod. Phys. **45**, 553 (1973).
[16] E. Y. Sidky and N. Andersen, Phys. Essays **13**, 489 (2000).
[17] J. H. Macek and S. Y. Ovchinnikov, Phys. Rev. Lett. **80**, 2298 (1998).